



Contents lists available at ScienceDirect

NeuroImage

journal homepage: www.elsevier.com/locate/ynimg

Phospholipase A₂ activity is associated with structural brain changes in schizophrenia

Stefan Smesny^{a,*}, Berko Milleit^a, Igor Nenadic^a, Christoph Preul^{a,c}, Daniel Kinder^a, Jürgen Lasch^b, Ingo Willhardt^b, Heinrich Sauer^a, Christian Gaser^a

^a Department of Psychiatry and Psychotherapy, Friedrich-Schiller-University Jena, Philosophenweg 3, D-07743 Jena, Germany

^b Department of Physiological Chemistry, Martin-Luther-University, Halle/Wittenberg, Hollystraße 1, D-06097 Halle, Germany

^c Department of Neurology, Friedrich-Schiller-University Jena, Erlanger Allee 101, D-07747 Jena, Germany

ARTICLE INFO

Article history:

Received 14 September 2009

Revised 3 May 2010

Accepted 5 May 2010

Available online xxxx

Keywords:

Schizophrenia

Imaging

MRI

Gray matter

White matter

Morphometry

Phospholipids

Membrane lipids

Marker

ABSTRACT

Regional structural brain changes are among the most robust biological findings in schizophrenia, yet the underlying pathophysiological changes remain poorly understood. Recent evidence suggests that abnormal neuronal/dendritic plasticity is related to alterations in membrane lipids. We examined whether serum activity of membrane lipid remodelling/repairing cytosolic phospholipase A₂ (PLA₂) were related to regional brain structure in magnetic resonance images (MRI). The study involved 24 schizophrenia patients, who were either drug-naïve or off antipsychotic medication, and 25 healthy controls. Using voxel-based morphometry (VBM) analysis of T1-high-resolution MRI-images, we correlated both gray matter and white matter changes with serum PLA₂-activity. PLA₂ activity was increased in patients, consistent with previous findings. VBM group comparison of patients vs. controls showed abnormalities of frontal and medial temporal cortices/hippocampus, and left middle/superior temporal gyrus in first-episode patients. Group comparison of VBM/PLA₂-correlations revealed a distinct pattern of disease-related interactions between gray/white matter changes in patients and PLA₂-activity: in first-episode patients ($n = 13$), PLA₂-activity was associated with structural alterations in the left prefrontal cortex and the bilateral thalamus. Recurrent-episode patients ($n = 11$) showed a wide-spread pattern of associations between PLA₂-activity and structural changes in the left (less right) prefrontal and inferior parietal cortex, the left (less right) thalamus and caudate nucleus, the left medial temporal and orbitofrontal cortex and anterior cingulum, and the cerebellum. Our findings demonstrate a potential association between membrane lipid biochemistry and focal brain structural abnormalities in schizophrenia. Differential patterns in first-episode vs. chronic patients might be related to PLA₂-increase at disease-onset reflecting localized regenerative activity, whereas correlations in recurrent-episode patients might point to less specific neurodegenerative aspects of disease progression.

© 2010 Elsevier Inc. All rights reserved.

Introduction

Regional brain structural changes are among the best replicated findings in schizophrenia (Honea et al., 2005; May and Gaser, 2006; McCarley et al., 1999; Shenton et al., 2001; Steen et al., 2006). Although research has considerably progressed in characterizing associations between structural changes, stage of disorder, severity of symptoms and treatment response, little is known about the underlying pathophysiology of structural alterations (DeLisi et al., 2004; Garver, 2006; Garver et al., 2000; Kasai et al., 2003; Scherk and Falkai, 2006; Velakoulis et al., 2002).

Gray matter changes have been identified in medial temporal lobe structures such as hippocampus, entorhinal and parahippocampal cortex, assumed to constitute a neuroanatomical correlate of vulner-

ability to develop schizophrenia (Chance et al., 2003; Falkai et al., 2002; Seidman et al., 2003). There is also evidence for frontal lobe changes, particularly in dorsolateral prefrontal and orbitofrontal regions, and for changes in the thalamus and basal ganglia, possibly arising subsequently to medial temporal lobe abnormalities (Harrison, 1999; McCarley et al., 1999).

The distributed pattern (and temporal evolution) of structural changes has been embedded in schizophrenia concepts focusing on circuitry abnormalities, affecting brain regions not necessarily in anatomical proximity to each other but nonetheless functionally interrelated (Andreasen et al., 1998; Weinberger and Lipska, 1995). From a brain structural perspective, the dysconnection concept is also supported by diffusion tensor imaging (DTI) and more recent multimodal imaging studies suggesting disruption of fiber tracts in white matter of the medial temporal lobe and other brain regions to be accompanied by neurochemical changes (Kubicki et al., 2007; Tang et al., 2007), as well as findings on oligodendrocyte pathology providing evidence for disturbed myelin maintenance and repair in schizophrenia (Davis et al., 2003).

* Corresponding author. Department of Psychiatry, Friedrich-Schiller-University Jena, Philosophenweg 3, D-07743 Jena, Germany. Fax: +49 3641 936697.

E-mail address: Stefan.Smesny@med.uni-jena.de (S. Smesny).

A common factor underlying structural changes in gray and white matter is molecular modification of cell membranes and myelin sheaths. This involves dynamic modeling including both synthesis and break-down of phospholipid bilayers. In fact, there is increasing evidence for disturbed membrane phospholipid metabolism in schizophrenia and particularly for disturbed activity of phospholipase A₂, the key regulating enzyme of phospholipid turnover. This group of enzymes is related to structural changes of gray and white matter in modifying lipid membranes. Likewise, it is related to a variety of processes known to be crucial in the pathophysiology of acute psychosis, such as monoaminergic imbalance, neurotoxicity, response to oxidative stress, dysapoptosis, neuroinflammation and a shifted immune response (Farooqui et al., 1999, 2004, 1997a,b; Taketo and Masahiro, 2002; Winstead et al., 2000). The group of phospholipase A₂ enzymes constitutes a “superfamily”, involving three major groups: (1) secretory (extracellular) Ca²⁺-dependent PLA₂ (sPLA₂); (2) cytosolic Ca²⁺-dependent PLA₂ (cPLA₂); and (3) intracellular Ca²⁺-independent PLA₂ (iPLA₂) (Balsinde et al., 1999; Dennis, 1994; Sun et al., 2004). Intracellular acting (cytosolic) PLA₂ enzymes occur ubiquitarily, are activated on demand, and are (as other serine esterases) able to pass the blood-brain barrier (Reiber, 2005). Once being activated, increased enzyme activity can be measured in blood serum and cerebrospinal fluid, and we have previously shown a close correlation of PLA₂ activity in serum and CSF (as obtained from lumbar puncture samples) in other patient cohorts (Smesny et al., 2008). The activity of PLA₂ measured in this study comprises cytosolic isoenzymes of groups (2) and (3).

Studies in serum samples as well as post mortem brain tissue have demonstrated an overall increase in intracellular PLA₂ activity (including cPLA₂ and iPLA₂ subtypes) compared to healthy controls (Gattaz et al., 1990, 1987, 1995; Lasch et al., 2003; Ross et al., 1997; Ross et al., 1999; Smesny et al., 2005; Tavares et al., 2003). Moreover, as a possible effect of increased PLA₂ activity, phospholipid fatty acids and phospholipids were also reduced in postmortem brain tissue from patients with schizophrenia (Horrobin et al., 1991; Yao et al., 2000). PLA₂ up-regulation was found particularly in the initial acute phase of disease onset (Smesny et al., 2005), and is at least partially ameliorated with antipsychotic medication, thus, paralleling the temporal course of some brain structural changes (Gattaz et al., 1990, 1987; Tavares et al., 2003).

As intracellular acting isotypes of PLA₂ are implicated in differentiation and proliferation of nervous tissue, intracellular membrane trafficking, oxidative stress, and apoptotic processes (Dennis, 1994; Sun et al., 2004; Taketo and Masahiro, 2002), we propose increase of PLA₂ activity at the time of first episode as a possible indicator of increased effort to maintain structural and functional integrity, potentially as compensatory process following a developmental deficit or neurotoxic effects of acute psychosis (Berger et al., 2006).

In this study we investigate relations between structural brain abnormalities and changes of phospholipid biochemistry in schizophrenia. We tested the hypothesis that brain structural changes in regions linked to schizophrenia (as identified with MRI) are related to lipid membrane remodeling and repair (mostly in gray matter) and myelin sheathing (white matter), for which PLA₂ is a crucial enzyme, thus being correlated to regional gray and/or white matter changes. For this purpose, we correlated PLA₂ activity with voxel based morphometry (VBM) measures obtained from T₁-weighted high-resolution MR-images. To additionally account for effects of stage of disorder we investigated both first-episode (FEP) and recurrent-episode (REP) patients in an age-corrected analysis and included only patients who were off antipsychotic medication or antipsychotic-naïve.

Methods

Subjects

We included 24 consecutively admitted patients from the inpatient unit of the Department of Psychiatry of University of Jena (all Caucasians,

epidemiologic data in Table 1) fulfilling DSM-IV criteria for schizophrenia or schizophreniform disorder. Diagnosis was established by two independent board-certified psychiatrists (St.S., H.S.) and confirmed by structured clinical interview (SCID IV) (Wittchen et al., 1997). Patients were sub-divided according to stage of illness, as the intensity of both PLA₂ alteration as well as focal brain structural changes have been shown to vary with the stage of disorder.

All patients presented with acute positive and negative symptoms at the time of investigation (see also Table 1); 13 patients suffered their first acute psychotic episode (FEP), of which 9 were neuroleptic-naïve and 4 free of neuroleptic medication; another 11 patients had recurrent acute psychotic episodes (REP), i.e. recovered from an acute psychotic episode, having had at least one previous psychotic episode (range: 2–4 total psychotic episodes, including the current) and had been in in- or outpatient psychiatric care for at least two years. Of those REP patients, two patients were still neuroleptic-naïve (having refused any neuroleptic medication so far) and 9 were off neuroleptic medication. All but two previously medicated patients were off antipsychotics for at least two weeks (time range of each subgroups, see Table 1); of the remaining two, one patient of the FEP and one of the REP groups had been free of medication for 5 days before inclusion (both previously treated with risperidone 4 mg/day, and thus off neuroleptics for more than 4 half-life times of this drug). As far as could be detected, FEP were (if pretreated) only treated with antipsychotic agents named in Table 1. In contrast, REP were during the course of their illness treated with divers antipsychotic agents including first generation neuroleptics such as haloperidol, flupentixol and perazine, and second generation neuroleptics such as risperidone, olanzapine, amisulprid and quetiapine. All REP had been intermittently treated with benzodiazepines, but none of them had been treated with clozapine before investigation.

Patients were compared to 25 healthy volunteers (C, all Caucasians, epidemiological data given in Table 1). Semi-structured interviews were used to assess current mental and medical status as well as personal and family history of any mental disorder. None of the controls had any personal or family history of psychiatric disorders including abuse of alcohol, cannabis or any other drug, or had any neurological or other somatic disorder affecting the CNS. Patients and controls did not suffer acute or chronic inflammatory diseases at the time point of measurement and were not recently treated with non-steroidal or steroidal anti-inflammatory drugs. This study was approved by the Research Ethics Committee of the Friedrich-Schiller-

Table 1
Epidemiological data and status of medication for each group.

	Controls	First episode patients	Recurrent episode patients
<i>Number (N), gender, age</i>			
N	25	13	11
Male/Female	10/15	6/7	1/10
Age (±SD) in years	35.31 (±10.59)	31.41 (±9.35)	46.42 (±9.65)
<i>Psychopathological ratings (±SD)</i>			
SAPS total		44.53 (20.21)	42.70 (18.07)
SANS total		40.17 (21.30)	38.24 (17.16)
<i>Neuroleptic medication (number of patients)</i>			
NL-naïve		9	2
NL-free (≥4 days), Range		4 (5 days–28 days)	9 (5 days–5 months)
<i>Previous medication (number of patients)</i>			
Risperidone		3	2
Olanzapine		0	4
Haloperidol		0	1
Perazine		0	1
Unknown		1	1

University Jena. All subjects gave written informed consent to participate in the study.

Acquiring and storage of blood samples

Venous blood (10 ml) was taken from an antecubital vein using a 19-gauge butterfly into a dry plastic syringe. Blood was allowed to clot for 30 min at room temperature. Serum was then separated by centrifugation (10 min at 3000g) and immediately stored in 1 ml aliquots at -35°C . In contrast to membrane fatty acids and phospholipids (Glen and Glen, 2004; Ross et al., 2004), follow-up measures to investigate stability of PLA₂ activity over time showed stability of quantitative analyses of enzyme activity for up to 5 years after blood sampling, if aliquots were stored continuously at -35°C , and provided that the thawed sera were re-centrifuged and stirred carefully in order to avoid any inhomogeneities of the specimen (Lasch et al., 2003). In this study, blood was taken right before the VBM investigation in most cases; in those cases with a time lag between MRI and blood sampling this did not exceed 2 days and is therefore not likely to have influenced results.

Analysis of PLA₂-activity

Serum PLA₂ activity was measured using the high performance thin layer chromatography (HPTLC) based fluorometric method described by Lasch and co-workers (Lasch et al., 2003). We used NBDC₆-HPC® (Molecular Probes Europe BV Leiden, The Netherlands) as fluorogenic substrate. A HPTLC based approach was favored as it allows separate measurements of substrate and product fluorescence. Hence, only PLA₂ catalyzed substrate degradation was measured. Specific enzyme activity is given in [pmol/min/mg protein].

As mentioned earlier, most of the intracellular acting PLA₂ enzymes need calcium in micromolar concentrations at most (cPLA₂) or are completely independent of calcium (iPLA₂). The classification of our target enzyme activity as *intracellular* is based on previous methodical investigations (Lasch et al., 2003) showing an almost complete (more than 90%) inhibitory effect of calcium ions on enzyme activity and a 70% inhibition of the enzyme activity by bromoenole lactone (BEL), a complete inhibitor of iPLA₂ (Jenkins et al., 2001; Lucas et al., 2005; Song et al., 2006; White and McHowat, 2007). As cPLA₂ has ubiquitary action with only micromolar calcium concentrations, it might also have contributed to the measured PLA₂ activity here. In contrast, previous research excluded the contribution of PAF-Hydrolases to the investigated activity, as PAF-hydrolases do not cleave the used commercial substrate. There was no reaction with PAF-Hydrolase antibodies (Lasch et al., 2003). Therefore, according to the most recent genetically defined classification, PLA₂ activity investigated in this study comprises mostly group IV and group VI type isoenzymes (Sun et al., 2004) and has been already used for previous investigations in schizophrenia patients (Lasch et al., 2003; Smesny et al., 2005).

Acquisition of structural data and image processing

We acquired high-resolution MRI on a 1.5 T Philips Gyroscan ACSII system (256 sagittal slices using a T1-weighted sequence (TR = 13 ms, TE = 5 ms, flip angle 25°) with isotropic voxel size of $1 \times 1 \times 1 \text{ mm}^3$). Data pre-processing and analysis was performed using Statistical Parametric Mapping (SPM8) software (Wellcome Department of Cognitive Neurology, London, UK). For morphometric analysis of the data we used voxel-based morphometry (VBM). This method involves the following steps: (i) spatial normalization of all images to a standardized anatomical space by removing differences in overall size, position, and global shape; (ii) extracting gray and white matter from the normalized images; and (iii) analyzing differences in local gray and white matter values across the whole brain (Ashburner and Friston, 2000). We applied an optimized method of VBM (Good et al., 2001)

using the VBM8 Toolbox (<http://dbm.neuro.uni-jena.de/vbm>) for both gray and white matter.

The segmentation procedure was further refined by accounting for partial volume effects (Tohka et al., 2004), by applying adaptive maximum a posteriori estimations (Rajapakse et al., 1997), and by applying a hidden Markov random field model (Cuadra et al., 2005), as described in Luders et al. (2009) (Luders et al., 2009). Because spatial normalisation expands and contracts some brain regions we scaled the segmented images by the amount of contraction, so that the total amount of gray or white matter in the images remains the same as it would be in the original images.

The resulting maps represent the local probability of belonging to a particular tissue type and reveal values between 0 and 1. Because we applied a nonlinear spatial registration the same voxel location in each image can be assumed to correspond to the same brain structure. By analyzing the probability values we examined the relative concentration of one tissue type (i.e. the proportion of gray matter to other tissue types within a region). We restricted the statistical analysis to areas with a minimum probability value of 0.1 to avoid possible edge-effects around tissue borders. The resulting gray and white matter images were finally smoothed with a Gaussian kernel of 12 mm FWHM.

Statistical analysis

Statistical analysis of PLA₂ activity was performed using the software package SPSS 15 for Windows. For evaluation of group differences, univariate analysis of variance (ANOVA) was performed using PLA₂-activity as dependent variable, GROUP as between-subject-factor and gender and age as co-variables. To further investigate group differences found significant in ANOVA we performed multiple pair-wise group comparisons using two-tailed Student's *t*-test at $p = 0.05$.

Group-wise comparison of *imaging data* was performed independently for gray and white matter using a general linear model implemented in the software package SPM8 (Statistical Parametric Mapping). To account for variance related to age effects (due to different mean age between FEP and REP) and gender effects we included age and gender as confounding variables into the model. We present only results of age and gender corrected analyses. Because of our anatomical hypothesis we set the significance threshold for resulting statistics at $p < 0.001$.

Assessment of associations between PLA₂ activity and structural abnormalities was performed using a general linear model in SPM8 with PLA₂ activity defined as co-variate. To account for age-related and gender effects we included age and gender as confounding variables into the model.

For pair-wise group comparison this type of analysis equals an interaction model testing for different regression slopes between gray/white matter density and PLA₂ activity in each voxel (PLA₂ activity by group interaction). Because variance was expected to differ between samples we applied non-sphericity correction. Again, all statistical images were thresholded at $p < 0.001$.

To support anatomical labeling we used the AAL toolbox (Tzourio-Mazoyer et al., 2002). For manual control of anatomical labeling we used the atlases of Nieuwenhuys (Nieuwenhuys et al., 2008) and of Mori (Mori et al., 2005).

Results

Sample characteristics and PLA₂ activity

There were differences in gender ratio and mean age between groups (Table 1). Group differences in mean age at time of investigation originate from the natural age of onset and the course of disease, leading to a consistently higher age in recurrent-episode patients (*t*-test: FEP vs. REP: $p = 0.001$, for C vs. REP: $p = 0.006$). We took this into account by

considering age as co-variate in all following analyses, thus assuring our findings are not due to mere effects of age. In terms of gender distribution, Fisher's exact test (gender by group) yielded $p = 0.252$ for C vs. FEP, 0.059 for C vs. REP and 0.055 for FEP vs. REP. Investigating a potential influence of epidemiological covariates on PLA₂ activity, univariate ANOVA and correlation analysis could not reveal any significant effect of gender or age on enzyme activity.

Univariate ANOVA resulted in significant effects of GROUP on PLA₂ activity ($F = 9.23$, $p < 0.001$, AGE and GENDER corrected model $F = 3.44$, $p = 0.008$). Performed t -tests showed that PLA₂ activity in both patient groups was higher than in controls (Table 2, Fig. 1; C vs. FEP: $p < 0.001$, C vs. REP: $p = 0.039$). Higher mean PLA₂ activity in FEP than in REP (difference of mean values: 159.08 pmol/min/mg protein) was not significant ($p = 0.119$) at this sample size.

VBM-based pair-wise group comparison of brain imaging data

Compared to controls, analysis of gray matter in FEP revealed reduced density in frontal (left superior and medial frontal gyrus; right inferior frontal/orbitofrontal gyrus) and temporal (left superior and medial temporal gyrus, left hippocampus; right superior temporal gyrus, temporal pole) brain regions. The REP group showed the same structural abnormalities, but in a more extensive pattern. In addition, analysis in REP also revealed areas of reduced gray matter in the insular cortex (left greater than right). Interestingly, REP showed a tendency of increased gray matter density in cerebellar brain regions.

Analysis of white matter group differences revealed in FEP mainly abnormalities in left hippocampal structures and at the posterior cingulum bundle. In REP, areas of reduced white matter involved also the regions of the globus pallidus and the internal capsule (crus posterior) as well as fronto-occipital, post-central (thalamocortical) and mesencephalic structures (cerebral peduncles). Comparison of white matter density between FEP and REP revealed especially marked abnormalities within the region of the cerebral peduncles, which (among others) includes long fiber tracts from the internal capsule (all results in more detail in Table 3).

Associations of PLA₂ activity and brain structure in healthy controls

In gray matter we identified one cluster (872 voxels, $T = 3.68$, $p = 0.043$), located in left parietal lobe showing a positive correlation between PLA₂ activity and gray matter. No other correlations between PLA₂ activity and brain structure were found in healthy controls.

VBM-based pair-wise group comparison of associations between PLA₂ activity and brain structure in schizophrenic patients and healthy controls

Comparing the PLA₂-gray matter (GM) and PLA₂-white matter (WM) correlations maps in either patient group to healthy controls (i.e. FEP vs. controls and REP vs. controls), we found significant effects in both cortical and subcortical areas. Note that each group comparison assesses the difference in association of PLA₂ to GM (or WM, resp.) between the groups, i.e. an interaction effect. Hence, Table 4a (for gray matter) and Table 4b (for white matter) indicate all significant interactions, while the figures additionally include plots of

Table 2
Results and corresponding statistical information of PLA₂ activity analysis, specified in pmol/min/mg protein.

	Control group	First episode patients	Recurrent episode patients
Range	203.97–930.81	366.85–1118.13	248.80–1009.62
Mean ± SD	506.14 ± 223.78	796.79 ± 178.39	673.71 ± 192.87
Median	513.79	823.01	667.66
95% Confidence interval	413.77–598.51	688.99–904.59	544.14–803.29

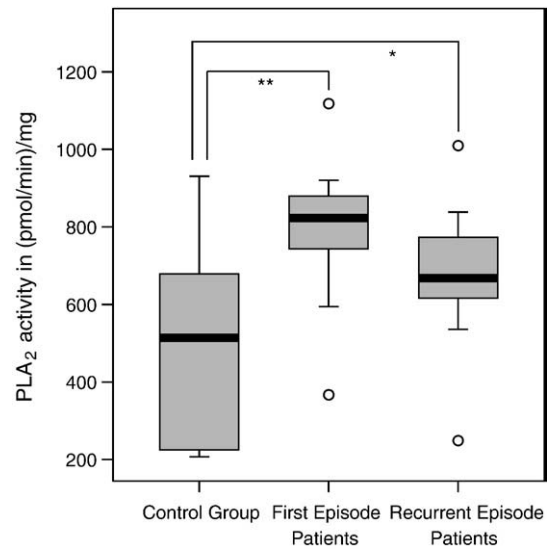


Fig. 1. SPSS generated boxplot for results of PLA₂ specific activity analysis. Black bar within box: median. Gray box: 25% to 75% quantile. Small black bars: minimum to maximum. Circles: outliers. Significant group differences are marked with * $p < 0.05$ and ** $p < 0.001$.

Table 3
Results of VBM group comparison of brain structure in controls vs. patient groups. C, FEP and REP are used as abbreviations for group names. Between-group differences regarding gray respective white matter were found in reported clusters. Only clusters showing group differences at a significance level of $p < 0.001$ and exceeding the expected number of voxels per cluster according to the Gaussian Random Field theory were reported. For each cluster anatomic labeling, corresponding cluster size and T -value are shown. Results for gray and white matter are presented separately. Type of group comparison is indicated in the form $A < > B$, whereby $A > B$ indicates lower gray/white matter in group B compared to A and vice versa. Lateralization is marked with L for left and R for right hemisphere.

Interaction	Anatomical Region	Cluster Size	T-value (voxel)
<i>VBM gray matter analysis of group differences</i>			
C > FEP	Frontal lobe. Inferior orbital gyrus. R	639	4.24
	Temporal lobe. Superior temporal pole. R	359	3.85
	Temporal lobe. Middle temporal gyrus. L	331	3.72
	Frontal lobe. Middle frontal gyrus. L	313	3.43
	Occipital lobe. Middle occipital gyrus. R	715	4.46
C < FEP	<i>No significant clusters</i>		
C > REP	Insula. R	753	4.17
	Insula. L	4281	4.34
	Frontal lobe. Inferior frontal gyrus. L		4.66
	Frontal lobe. Inferior frontal gyrus. L		4.15
	Temporal lobe. Superior temporal gyrus. L	946	4.52
	Frontal lobe. Superior frontal gyrus. R	445	4.50
	Frontal lobe. Precentral gyrus. R	282	4.32
C < REP	Cerebellum. R	812	4.03
FEP > REP	Insula. R	427	3.97
FEP < REP	Cerebellum. R	2513	4.29
	Cerebellum. L	333	3.82
	Occipital lobe. Cuneus. L	895	4.56
<i>VBM white matter analysis of group differences</i>			
C > FEP	<i>No significant clusters</i>		
C < FEP	Cingulum bundle. L	553	4.72
C > REP	Cerebral peduncle. R	1895	4.09
	Cerebral peduncle. L	418	3.77
	Posterior limb of inner capsule. L	433	3.62
	Occipital lobe / fronto-occipital fasciculus. L	534	4.07
C < REP	Postcentral white matter/superior thalamic radiation	223	2.82
FEP < REP	Cerebral peduncles. LR	9143	4.47
FEP > REP	<i>No significant clusters</i>		

Table 4a

Results of VBM-based pair-wise group comparison of associations between PLA₂ activity and brain structure (VBM based interaction analysis; Co-variate: PLA₂; nuisance variables: gender, age). Clusters showing significant group differences regarding correlations between PLA₂ activity and **gray matter** density. All results are presented separately for region (cortical structures and white matter) and type of analysis (gray matter and white matter analysis). Type of interaction analysis is indicated in the form A</>B. A>B indicates a significantly steeper gradient of regression of A as compared to B and vice versa. C, FEP and REP are used as abbreviations for group names. Only clusters showing group differences at a significance level of $p = 0.001$ are reported. For each cluster corresponding cluster size, *T*-value, and coordinates are shown. For all cluster >10 voxel corresponding anatomical regions (parts >10% of cluster size) are shown as determined by AAL-software (Anatomical Automatic Labeling) for SPM, each manually checked by the investigators according to the atlas by Nieuwenhuys et al. (2008), Nieuwenhuys et al. (2008), Mori et al. (2005) and by Mori et al. (2005). Clusters are numbered for easier identification in tables, figures and text sections. Those clusters corresponding to clusters presented in figures are printed in bold.

Results derived from grey matter analysis							
Type of interaction	Cluster number	Cluster size (voxels)	<i>T</i> -value	<i>p</i> -value	Coordinates	Region	
C > FEP	1	13	3.64	0.000	−48 15 18	Left prefrontal, G. frontalis inferior	
	2	7	3.59	0.000	−41 8 −30		
	3	7	3.46	0.000	42 9 −33		
	4	7	3.43	0.001	−3 −78 45		
FEP > C	5	93	4.98	0.000	20 −88 −2	Right inferior posterior lobe	
	6	56	4.49	0.000	35 −42 −44	Right cerebellum, anterior lobe	
	7	64	4.47	0.000	−38 −75 25	Left inferior parietal lobule	
	8	75	4.43	0.000	36 −88 30	Right inferior parietal lobule	
	9	30	4.18	0.000	−9 −10 1	Left anterior thalamus	
	10	38	3.90	0.000	44 −4 60	Right precentral gyrus	
	11	50	3.81	0.000	−51 −13 52	Left postcentral gyrus, anterior bank	
	12	34	3.75	0.000	−11 −15 −26	Left cerebral peduncle	
	13	15	3.56	0.000	12 −36 73	Right superior precentral gyrus	
	14	9	3.53	0.001	17 −3 51		
	15	5	3.42	0.001	45 −37 51		
	16	4	3.35	0.001	3 21 6		
	17	4	3.34	0.001	−35 −45 −48		
	18	1	3.32	0.001	−15 24 34		
C > REP	19	244	4.97	0.000	48 41 27	Right middle frontal gyrus, middle 1/3	
	20	84	4.71	0.000	29 −63 −0	Right parahippocampal gyrus	
	21	63	4.37	0.000	9 −51 −32	Right paramedian anterior cerebellar lobule	
	22	173	4.26	0.000	−29 −76 43	Left inferior parietal lobule	
	23	123	4.19	0.000	−62 −46 −6	Left medial temporal gyrus, middle 1/3	
	24	6	4.10	0.000	−48 −36 −14	Left medial temporal gyrus, middle 1/3	
	25	170	4.06	0.000	−18 45 21	Left superior frontal gyrus, anterior 1/3	
	26	32	3.94	0.000	−17 −51 30	Left precuneus	
	27	58	3.86	0.000	30 −72 43	Right inferior parietal lobule	
	28	32	3.82	0.000	−35 −69 30	Left inferior parietal lobule	
	29	21	3.69	0.000	39 60 4	Right medial frontal gyrus	
	30	16	3.63	0.000	−20 −78 25	Left parietal-occipital transition / cuneus	
	31	9	3.56	0.000	−3 −28 −14		
	32	25	3.49	0.001	−44 −66 36	Left inferior parietal lobule	
	33	4	3.46	0.001	−35 −13 −27		
	34	1	3.33	0.001	32 −42 56		
	REP > C	35	147	5.27	0.000	23 −27 13	Right posterior thalamus, close to fornical system
		36	210	4.48	0.000	18 −87 −2	Left medial occipital (lingual) gyrus
37		912	4.45	0.000	3 6 64	Right frontomedian F1, supplemental motor area SMA	
38		48	4.25	0.000	11 −82 45	Right cuneus	
39		974	4.16	0.000	51 −54 −50	Posterior cerebellar lobe	
40		43	4.14	0.000	38 −76 −12	Right inferior lateral occipital lobe	
41		61	4.09	0.000	−3 −66 −24	Left paramedian cerebellum	
42		112	4.04	0.000	−15 −18 −23	Left hippocampus formation	
43		196	4.01	0.000	−24 −42 −50	Left inferior cerebellum	
44		15	3.99	0.000	17 −3 52	Right superior frontal gyrus	
45		145	3.79	0.000	18 −10 27	Body of caudate nucleus right	
46		23	3.78	0.000	5 −96 27	Right cuneus	
47		58	3.76	0.000	3 21 54	Right superior frontal gyrus, median wall: SMA	
48		31	3.75	0.000	−23 −57 −57	Left inferior cerebellum	
49		111	3.70	0.000	−24 −70 −38	Cerebellar inferior semi-lunar lobe	
50		17	3.66	0.000	−11 −15 76	Left superior frontal gyrus	
51		16	3.54	0.001	41 −34 63	Right postcentral gyrus, posterior bank	
52		6	3.49	0.001	23 −75 56		
53	5	3.38	0.001	38 47 −20			
54	2	3.36	0.001	−32 29 −15			
55	1	3.34	0.001	−20 −7 24			
56	1	3.33	0.001	18 −6 −14			
FEP > REP	57	170	5.13	0.000	−18 36 22	Left superior frontal gyrus, lateral bank	
	58	377	5.00	0.000	−38 −75 25	Left inferior parietal lobule	
	59	181	4.80	0.000	33 −76 37	Right inferior parietal lobule, precuneus	
	60	104	4.65	0.000	32 −57 −2	Right temporooccipital gyrus	
	61	96	4.62	0.000	8 −51 −30	Right paramedian anterior cerebellar lobule	
	62	101	4.43	0.000	59 −16 −3	Right superior temporal gyrus, middle 1/3	
	63	176	4.29	0.000	45 41 28	Right middle frontal gyrus	
	64	18	3.96	0.000	−8 −10 −0	Left anterior thalamus	
	65	45	3.95	0.000	39 11 21	Foot region of middle frontal gyrus	
	66	24	3.90	0.000	42 −3 39	Right precentral gyrus, anterior bank	

(continued on next page)

Table 4a (continued)

Results derived from grey matter analysis						
Type of interaction	Cluster number	Cluster size (voxels)	T-value	p-value	Coordinates	Region
	67	6	3.77	0.000	−9 −1 −2	
	68	3	3.68	0.000	−33 −13 −27	
	69	2	3.50	0.001	−47 −49 −3	
	70	5	3.43	0.001	−39 −82 −5	
	71	3	3.38	0.001	−15 26 34	
	72	7	3.37	0.001	33 −42 56	
	73	8	3.35	0.001	−50 −16 34	
	74	4	3.34	0.001	30 −48 51	
REP > FEP	75	83	5.45	0.000	23 −28 15	Right posterior lateral thalamus / fornix
	76	75	4.59	0.000	27 −61 63	Right superior parietal lobule
	77	274	4.42	0.000	9 −72 −50	Right paramedian posterior cerebellar lobule
	78	44	4.33	0.000	−48 14 18	Left inferior frontal gyrus
	79	130	4.20	0.000	42 11 −35	Right temporal pole
	80	447	4.18	0.000	−8 −76 −44	Left paramedian posterior cerebellar lobule
	81	209	4.04	0.000	0 29 −12	Bilateral frontobasal paramedian, basis of cingulate gyrus
	82	84	3.71	0.000	54 −59 −45	Right lateral cerebellar region
	83	38	3.67	0.000	−2 32 9	Left anterior cingulate gyrus
	84	83	3.66	0.000	−12 −7 22	Left corpus of caudate nucleus
	85	30	3.65	0.000	23 −82 −14	Right temporooccipital lingual gyrus
	86	25	3.63	0.000	−66 −31 36	Left inferior parietal lobe
	87	7	3.59	0.000	−14 68 18	
	88	22	3.59	0.000	3 2 54	Right median frontal wall: SMA
	89	3	3.56	0.000	33 26 −29	
	90	30	3.50	0.001	3 23 55	Right median frontal wall: SMA
	91	2	3.48	0.001	−60 12 19	
	92	14	3.45	0.001	68 −40 31	Right inferior parietal region
	93	11	3.44	0.001	−2 −72 12	Left (basal) cuneus
	94	1	3.43	0.001	−60 −6 −36	
	95	2	3.40	0.001	59 −64 −17	
	96	1	3.38	0.001	−20 14 66	
	97	1	3.34	0.001	−18 48 −24	
	98	1	3.34	0.001	−20 0 −44	
	99	2	3.33	0.001	2 −3 67	
	100	1	3.33	0.001	−20 3 −45	
	101	1	3.33	0.001	−54 −54 −38	
	102	2	3.32	0.001	−17 −27 −18	

the associations to allow identification of the direction of associations, i.e. whether the interaction is caused by positive or negative correlations of PLA₂ with gray matter (Figs. 2 and 3) or white matter (Figs. 4 and 5) in patient groups. Clusters are numbered for easier identification across text, tables, and figures. We have also observed, in several cases, that focal cortical grey matter reductions were accompanied by adjacent white matter increase (and vice versa). Therefore, we manually checked localization of every cluster to assign it to cortical/subcortical structure or white matter tracts.

The main results of gray matter (GM) analysis are:

- (1) *FEP vs. Controls*: For the FEP vs. controls contrast for gray matter, we found significant interactions in the left ventral thalamus (cluster no. 9, see Table 4a and Fig. 2) as well as left inferior frontal cortex (cluster no. 1, Table 4a, Fig. 2). Additionally we found significant interactions in left (cluster 7) and right (cluster 8) inferior parietal and the right inferior posterior lobe (cluster 5), and in the right anterior cerebellum (cluster 6).
- (2) *REP vs. Controls*: For the REP vs. controls contrast for gray matter, we found significant interactions in both left superior frontal (cluster 25) and right middle frontal (clusters 19 and 29) cortex (see Table 4a and Fig. 2), the right posterior thalamus (cluster 35) the right caudate nucleus (cluster 45), as well as the left hippocampus formation (cluster 42) and medial temporal cortex (cluster 23), right parahippocampal gyrus (cluster 20) and several cerebellar clusters (esp. clusters 21, 39 and 49). As in FEP, we found again clusters in left inferior parietal (cluster 22, 28, and 32) and right inferior parietal (cluster 27) regions. Note that, unlike the FEP vs. controls

contrast, we found bilateral (left > right) frontal clusters in the REP vs. controls contrast.

- (3) *FEP vs. REP*: We also computed a FEP vs. REP contrast to assess potential differences between first-episode vs. multi-episode/chronic patients for gray matter, which (although all data is cross-sectional) might disclose differences related (at least in part) to effects of disease stage.

Of particular interest in the FEP vs. REP contrast (see Table 4a and Fig. 3) are clusters of significant interactions in the left superior frontal (cluster 57) and right middle frontal (cluster 63, 65) gyrus, the left (cluster 58) and right (cluster 59) inferior parietal cortex, left anterior (cluster 64) and right posterior lateral (cluster 75) thalamus, left caudate (cluster 84), and the cerebellum (clusters 61, 77 and 80). In addition, we found several large significant clusters in anatomical areas not observed in either FEP vs. controls or REP vs. controls contrasts; these included the left medial orbitofrontal and entorhinal cortex, and the left anterior cingulate cortex (clusters 81 and 83). The FEP vs. REP contrast included also several significant clusters in the right hemisphere, such as the parahippocampal gyrus (cluster 60), superior temporal gyrus (cluster 62), and temporal pole (cluster 79).

- (4) *Direction of interactions in the gray matter analyses*: While the above analyses of interaction (i.e. differences in association between PLA₂ and gray matter between the contrasted groups) show the anatomical areas of differences, we additionally investigated the direction of associations (correlations). These are given in the plot diagrams for clusters in Figs. 2 and 3 (for white matter in Figs. 4 and 5).

Table 4b

Results of VBM-based pair-wise group comparison of associations between PLA₂ activity and brain structure (VBM based interaction analysis; Co-variate: PLA₂; nuisance variables: gender, age). Clusters showing significant group differences regarding correlations between PLA₂ activity and **white matter** density. All results are presented separately for region (cortical structures and white matter) and type of analysis (gray matter and white matter analysis). Type of interaction analysis is indicated in the form A</>B. A>B indicates a significantly steeper gradient of regression of A as compared to B and vice versa. C, FEP and REP are used as abbreviations for group names. Only clusters showing group differences at a significance level of $p = 0.001$ are reported. For each cluster corresponding cluster size, T -value, and coordinates are shown. For all cluster >10 voxel corresponding anatomical regions (parts >10% of cluster size) are shown as determined by AAL-software (Anatomical Automatic Labeling) for SPM, each manually checked by the investigators according to the atlas by Nieuwenhuys et al. (2008), Nieuwenhuys et al. (2008), Mori et al. (2005) and by Mori et al. (2005). Clusters are numbered for easier identification in tables, figures and text sections. Those clusters corresponding to clusters presented in figures are printed in bold.

Results derived from white matter analysis							
Type of interaction	Cluster number	Cluster size (voxels)	T -value	p -value	Coordinates	Region	
C > FEP	103	56	4.76	0.000	45 – 15 42	Posterior bank of precentral gyrus	
	104	51	3.95	0.000	53 – 24 48	Right WM stalk of postcentral gyrus	
	105	53	3.87	0.000	41 – 48 43	Right inferior parietal lobule	
	106	3	3.51	0.001	– 30 – 12 67		
	107	13	3.42	0.001	33 – 33 46	Right WM stalk of postcentral gyrus	
	108	3	3.42	0.001	23 – 69 – 5		
	109	4	3.41	0.001	– 48 – 31 52		
	110	1	3.34	0.001	53 – 34 31		
	111	2	3.33	0.001	21 – 30 69		
	FEP > C	112	1058	4.96	0.000	3 – 12 1	Bilateral antero-medial thalamus, left dorsolateral thalamus, reaching up to body of caudate nucleus
		113	27	3.63	0.000	17 – 45 – 23	Right quadrangular cerebellar lobule;
114		5	3.54	0.001	– 20 – 81 – 41		
115		8	3.41	0.001	– 38 – 78 – 2		
116		2	3.39	0.001	6 2 – 12		
117		1	3.38	0.001	8 3 – 14		
118		1	3.33	0.001	– 41 – 78 33		
C > REP		119	72	4.66	0.000	– 57 – 54 – 11	Intersection between left medial and inferior temporal gyrus
	120	305	4.38	0.000	– 38 11 – 35	Left temporal pole region	
	121	23	3.89	0.000	59 – 37 – 24	Right WM stalk of inferior temporal gyrus	
	122	12	3.79	0.000	45 – 75 19	Right lateral temporo-occipital WM compartment	
	123	27	3.76	0.000	29 5 – 39	Right temporal medial pole region	
	124	15	3.53	0.001	51 12 – 26	Right WM stalk of superior temporal gyrus	
	125	15	3.48	0.001	57 – 31 18	Right WM stalk of superior temporal gyrus	
	126	6	3.40	0.001	– 18 – 70 25		
	127	1	3.31	0.001	32 – 58 – 53		
	128	1	3.30	0.001	– 8 – 63 36		
	REP > C	129	881	4.55	0.000	18 – 52 – 30	Right anterior cerebellar lobule / quadrangular lobule, reaching region of cerebellar peduncle and dentate nuclei
130		288	4.07	0.000	29 – 40 9	Right parieto-temporal white matter compartment (junction); involving tapetum and optic radiation	
131		22	3.89	0.000	11 – 70 45	Right precuneus, subparietal WM	
132		189	3.72	0.000	– 15 36 4	Left (pre-)cingulate white matter; forceps minor	
133		29	3.60	0.000	8 – 49 – 53	Right paramedian inferior cerebellum	
134		42	3.56	0.000	24 21 4	Right frontolateral white matter	
135		12	3.47	0.001	– 17 18 13		
136		4	3.45	0.001	24 – 12 52		
137		5	3.44	0.001	33 – 42 – 38		
138		6	3.41	0.001	0 – 16 – 5		
139		12	3.38	0.001	– 17 24 – 8	Left frontobasal white matter adjoining head of caudate nucleus	
140		3	3.36	0.001	20 45 – 15		
141		2	3.34	0.001	– 33 48 – 14		
142		1	3.31	0.001	– 21 30 – 11		
143		1	3.30	0.001	– 26 33 – 9		
FEP > REP		144	42	4.48	0.000	47 – 73 22	Right temporo-occipital region
		145	183	4.43	0.000	– 32 6 – 42	Left temporal pole
	146	40	4.07	0.000	32 – 58 – 53	Right inferior cerebellum	
	147	21	3.86	0.000	– 59 – 42 1	Right WM stalk of medial temporal gyrus	
	148	6	3.83	0.000	– 57 – 54 – 11		
	149	62	3.82	0.000	– 59 – 16 – 12	Left middle temporal gyrus anterior 1/3	
	150	58	3.77	0.000	8 – 12 9	Right anterior medial thalamus	
	151	81	3.74	0.000	– 8 – 57 31	Left subparietal region, precuneus	
	152	8	3.64	0.000	– 41 – 78 33		
	153	1	3.58	0.000	– 5 – 67 19		
	154	4	3.48	0.001	27 3 – 39	Right temporal medial pole region	
155	7	3.41	0.001	32 – 93 7			
156	7	3.39	0.001	– 38 – 79 – 5			
157	2	3.37	0.001	– 47 – 64 – 6			
REP > FEP	158	103	5.12	0.000	47 – 28 46	Right posterior bank of postcentral gyrus	
	159	321	4.06	0.000	– 17 33 13	Left anterior cingulum, Forceps minor	
	160	70	3.91	0.000	42 – 49 42	Right inferior parietal lobule	
	161	41	3.90	0.000	35 – 42 – 6	Right temporal white matter	
	162	3	3.47	0.001	60 – 30 27		
	163	4	3.41	0.001	44 – 16 42		

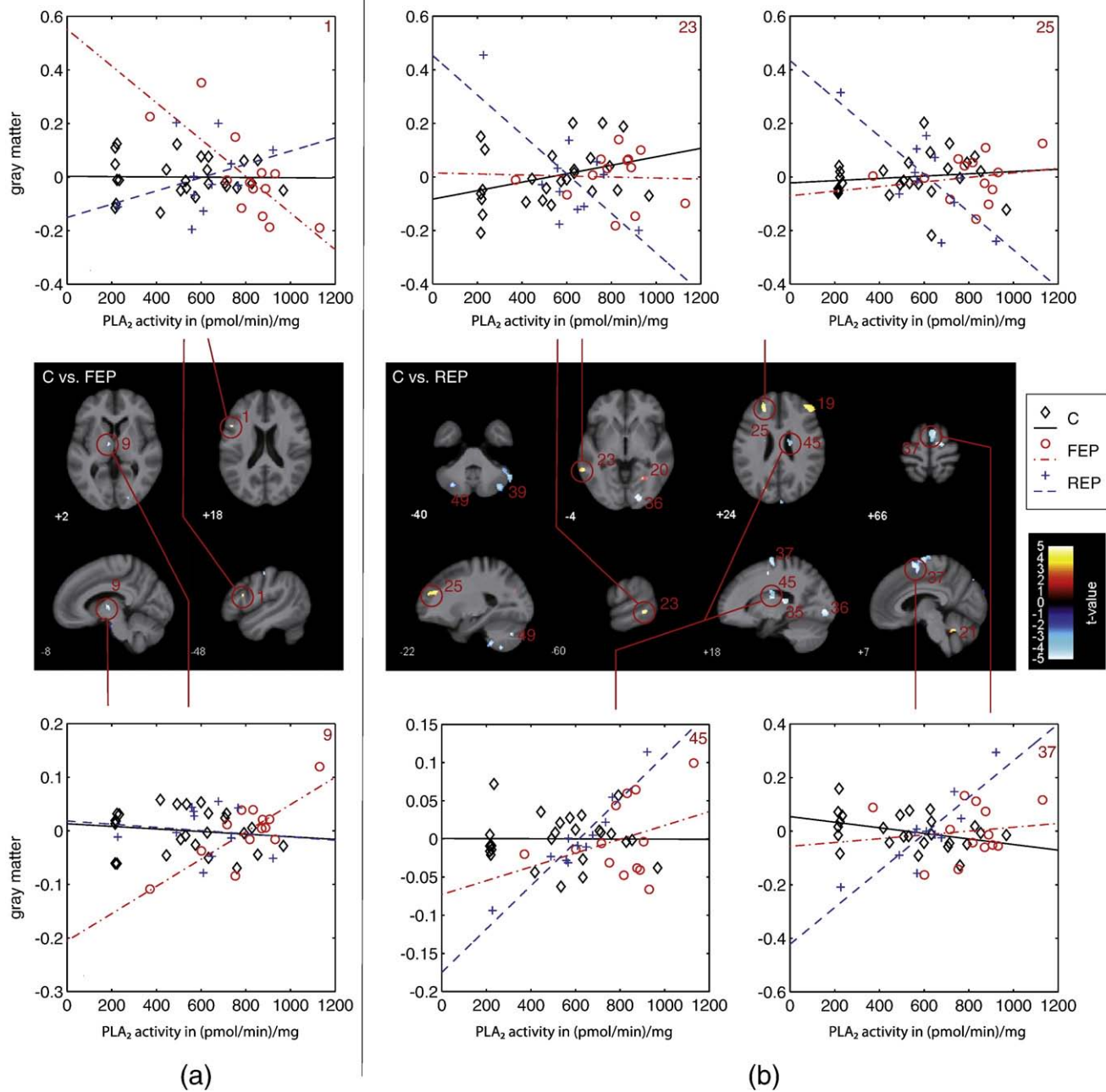


Fig. 2. Presentation of VBM-based pair-wise group comparison of associations between PLA₂ activity and **gray matter**. This figure shows the FEP vs. C, (a) and REP vs. C (b) contrast. Clusters shown are significant as stated and numbered in Table 4a and are shown as overlay onto the T1 average image in axial and sagittal plane for each group comparison as indicated below anatomical images. A T1 average image was generated from single images of all participants of this study. Positive interaction (slope of regression curve steeper in controls than in FEP or REP, or steeper in FEP than in REP) is marked by red/yellow color, negative interaction (slope of regression curve steeper in FEP or REP than in controls, or steeper in REP than in FEP) by blue color (colorbar with corresponding T-values in the upper right). Scatter plots showing PLA₂ activity against gray matter values (obtained from 1st Eigenvariate of its corresponding cluster) and corresponding regression lines are demonstrated exemplary for each found interaction pattern. Gray: controls (C); red: first episode patients (FEP); blue: recurrent episode patients (REP). Color and symbol codings are also shown within the figure on the right side.

In first-episode patients (FEP), for example, the left prefrontal cluster (figure 2, cluster 1) showed a negative correlation of GM with PLA₂ activity (i.e. the higher PLA₂ activity, the lower gray matter density), while the anterior thalamus cluster (cluster 9) showed a positive correlation (i.e. the higher PLA₂ activity, the higher gray matter density).

In repeated-episode patients (REP), we also identified both negative correlations (e.g. in bilateral frontal (clusters 19, 25) and inferior parietal (clusters 27, 28) regions, left medial temporal (cluster 23), and right parahippocampal gyrus (cluster 20)) indicating decreasing substance density with increasing PLA₂ activity, and positive correlations (e.g. right posterior thalamus (cluster 35), right caudate nucleus (cluster 45), and cerebellar clusters (39,49)), indicating the opposite association; see Fig. 2.

Comparing the patient groups directly (FEP vs. REP contrast), several of the clusters we had identified showed a positive correlation of PLA₂ with gray matter in FEP, but negative correlation of PLA₂ with gray matter in REP (e.g. bilateral frontal (Fig. 3, clusters 57, 63) and inferior parietal (clusters 58, 59) cortex, left anterior thalamus (cluster 64), right superior temporal cortex (cluster 62)). However, there were also significant clusters with the opposite pattern of correlations (i.e. negative correlation in FEP but positive correlation in REP), such as the left orbitofrontal and anterior cingulate cortex (cluster 81, 83), the left caudate nucleus (clusters 84), right temporal polar cortex (cluster 79) and bilateral cerebellum (clusters 77, 80, and 82; all Fig. 3).

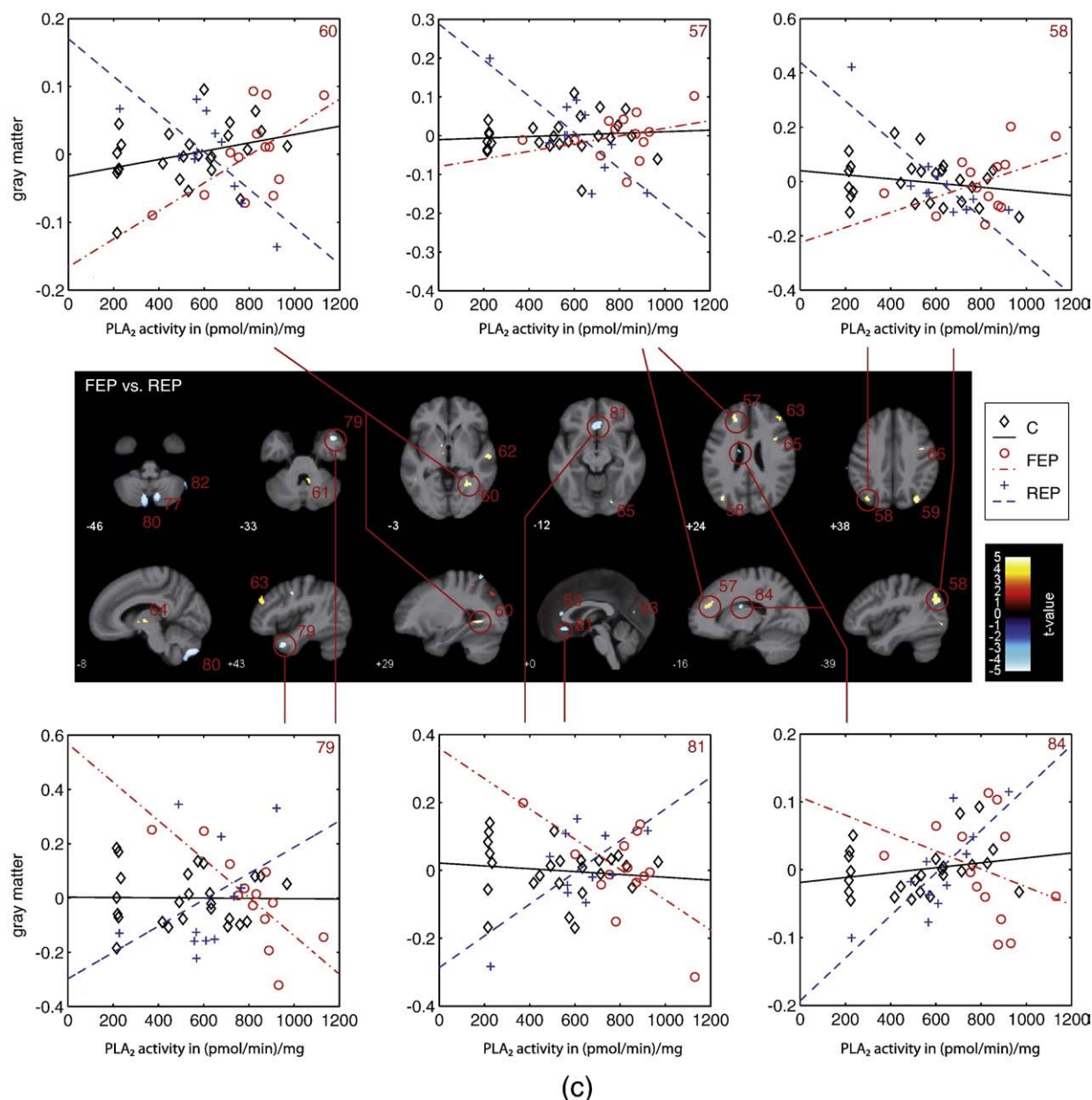


Fig. 3. Presentation of VBM-based pair-wise group comparison of associations between PLA_2 activity and **gray matter**. This figure shows the FEP vs. REP (c) contrast. Clusters shown are significant as stated and numbered in Table 4a and are shown as overlay onto the T1 average image in axial and sagittal plane for each group comparison as indicated below anatomical images. A T1 average image was generated from single images of all participants of this study. Positive interaction (slope of regression curve steeper in controls than in FEP or REP, or steeper in FEP than in REP) is marked by red/yellow color, negative interaction (slope of regression curve steeper in FEP or REP than in controls, or steeper in REP than in FEP) by blue color (colorbar with corresponding T-values in the upper right). Scatter plots showing PLA_2 activity against gray matter values (obtained from 1st Eigenvariate of its corresponding cluster) and corresponding regression lines are demonstrated exemplarily for each found interaction pattern. Gray: controls (C); red: first episode patients (FEP); blue: recurrent episode patients (REP). Color and symbol codings are also shown within the figure on the right side.

The main results of white matter (WM) analysis are:

- (1) *FEP vs. Controls*: Contrasting FEP vs. healthy controls for white matter associations with PLA_2 activity, we found a large cluster extending from the left anterior medial thalamus bilaterally and left dorsolateral thalamus extending towards the body of the caudate nucleus (cluster 112, Table 4b, Fig. 4). Smaller clusters were found at the right precentral (cluster 103) and (similar to GM-analysis in FEP) inferior parietal (cluster 105) gyrus and the right cerebellum (cluster 113).
- (2) *REP vs. Controls*: Contrasting REP vs. healthy controls for white matter associations with PLA_2 activity, we identified clusters adjacent to the gray matter findings, such as left medial temporal gyrus (cluster 119, Fig. 4) and cerebellar areas (cluster 129). But we found also significant clusters in left orbitofrontal white matter and anterior cingulum (cluster 132), in the left frontobasal white matter and anterior cingulum (cluster 139), and in the left (cluster 120) and right (cluster 123) temporal pole areas. There were several right hemispherical clusters, as in the right frontolateral white matter (cluster 134), the WM stalks of superior (clusters 124, and 125), and inferior (cluster 121) temporal gyrus, and the right parieto-temporal white matter (cluster 130).
- (3) *FEP vs. REP*: The contrast of FEP vs. REP patients for white matter yielded significant clusters of interaction in left anterior middle temporal area (cluster 149, Fig. 5) left temporo-occipital (cluster 144), temporal pole (cluster 145), left subparietal region (precuneus) (cluster 151) and left anterior cingulum and forceps

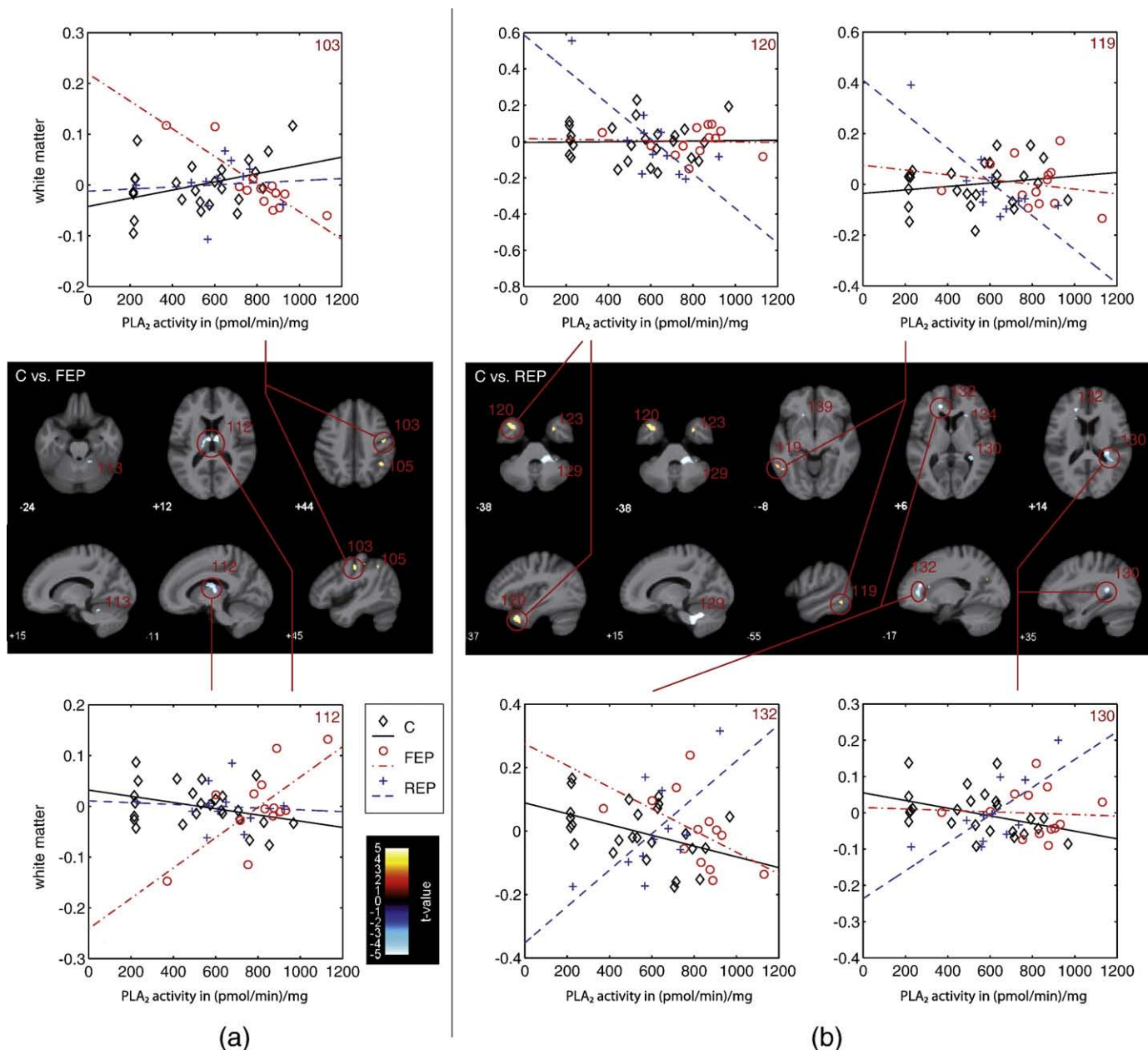


Fig. 4. Presentation of VBM-based pair-wise group comparison of associations between PLA₂ activity and **white matter**. This figure shows the FEP vs. C (a), and REP vs. C (b) contrast. Demonstration of results as in Figs. 2 and 3. Scatter plots showing white matter values (obtained from 1st Eigenvariate of the cluster).

minor (cluster 159). Right-hemispherical clusters included the anterior medial thalamus (cluster 150), WM stalk of medial temporal gyrus (cluster 147), temporal (cluster 161), postcentral (cluster 158) and inferior parietal (cluster 160) white matter. The large cluster in the left anterior cingulum (cluster 159, Fig. 5) parallels the findings of gray matter in the FEP vs. REP analysis, and in this particular region (see Fig. 3, clusters 83 and 81).

- (4) *Direction of interactions in the white matter analyses:* Similar to the gray matter analysis, we also observed different directions of correlations and thus different patterns of significant interactions for white matter clusters, as seen in the correlation plots (Figs. 4 and 5).

In the FEP vs. healthy controls contrast for white matter, there was a positive correlation of white matter density and PLA₂ activity in the thalamic clusters bilaterally (Fig. 4, cluster 112) and cerebellum (Fig. 4, cluster 113), i.e. FEP showing higher white matter density in

these clusters with increasing PLA₂ activity, but an opposite patterns (lower white matter density with increasing PLA₂ activity) for the postcentral and parietal clusters (103 and 105, resp.).

In the REP vs. healthy controls contrast for white matter, there was in REP a positive correlation of white matter density and PLA₂ activity in the anterior cingulum (cluster 132) and right cerebellum (cluster 129), but a negative correlation of white matter density and PLA₂ activity in the medial temporal area (cluster 119) and left temporal pole area (cluster 20; to a smaller degree also in the right temporal pole area, cluster 23).

In the FEP vs. REP contrast for white matter, we also found markedly different patterns of PLA₂-WM-associations (see Fig. 5). We found a positive correlation in FEP patients, but negative correlation in REP patients between white matter density and PLA₂ activity in the left medial temporal area (cluster 149), left temporal pole (cluster 145), and right thalamus (cluster 150). Only in the right cerebellum (cluster 159) did we find an opposite pattern, i.e. a

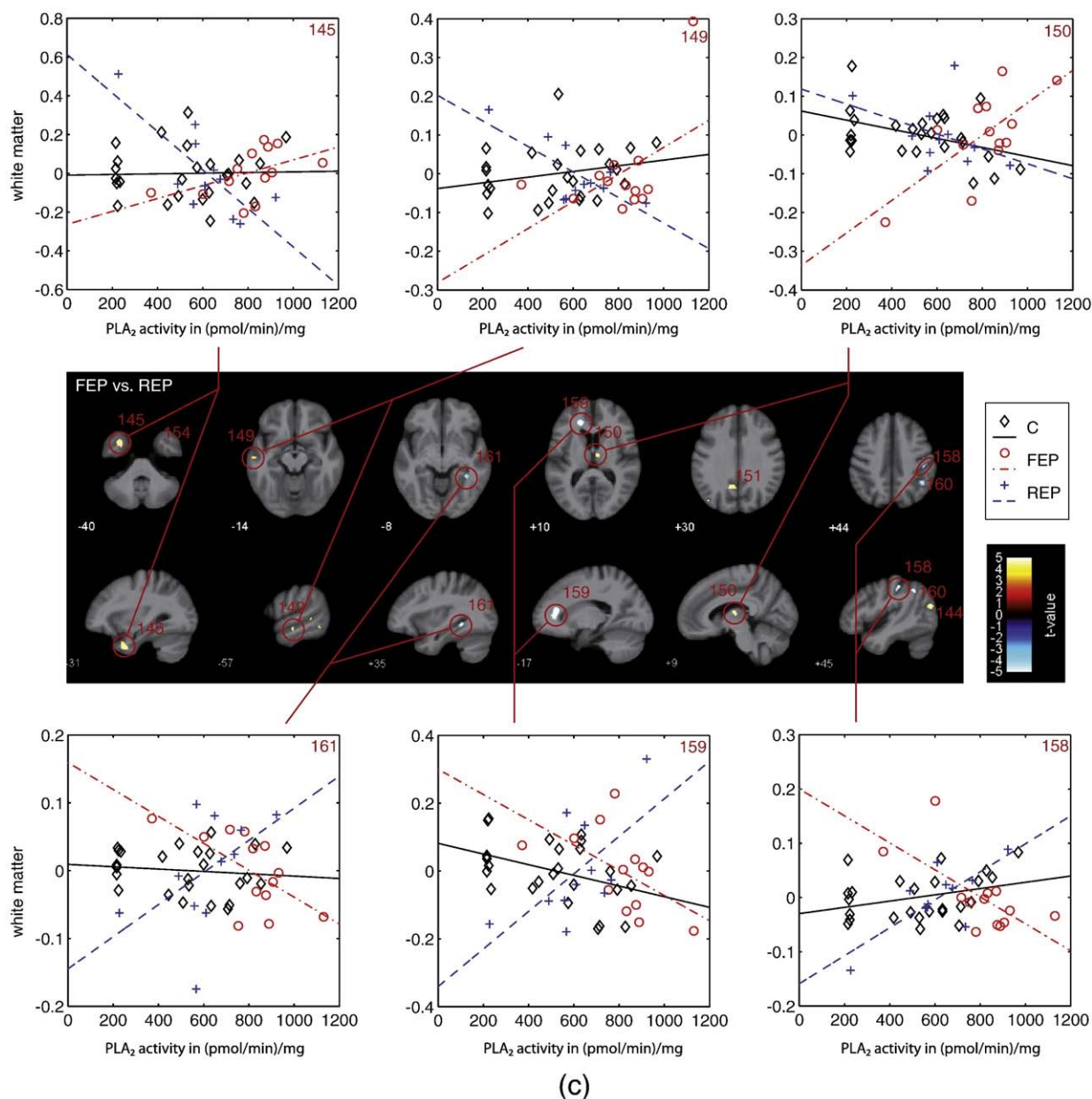


Fig. 5. Presentation of VBM-based pair-wise group comparison of associations between PLA₂ activity and white matter. This figure shows the FEP vs. REP contrast (c). Demonstration of results as in Figs. 2 and 3. Scatter plots showing white matter values (obtained from 1st Eigenvariate of the cluster).

negative WM–PLA₂ correlation in FEP, but positive WM–PLA₂ correlation in REP patients.

Discussion

In this study we analyzed both gray matter (GM) and white matter (WM) in two groups of schizophrenia patients at different stages of disease (first-episode vs. repeated-episode/chronic) and healthy controls, and we analyzed the correlation of local GM and WM with PLA₂ enzymatic activity in serum. Our study is one of the first studies to provide a link between morphometric abnormalities in schizophrenia and a putative biochemical marker, which gives potential insight into the pathology underlying brain structural changes in schizophrenia.

Our findings support the hypothesis, that PLA₂ activity is associated with and thus possibly modulating certain regional brain structural changes in schizophrenia. The interpretation of the results, however, needs to consider several important aspects. Firstly, PLA₂ has been implicated both in the breakdown as well as plasticity and

regeneration (e.g. remodelling) of phospholipid membranes. It is therefore important to distinguish its roles and in particular its involvement at different stages of the disorder. Previous studies of PLA₂ in serum of schizophrenia patients indeed indicate higher activity during the first episode of the disorder, and then a decrease (although still higher than in healthy controls) over the subsequent years (Smesny et al., 2005). This result could be confirmed in the present study. Since our data are cross-sectional, we need to rely on the comparison of FEP with REP patients to take into account this effect of disease stage. Secondly, our analyses of interaction between the GM–PLA₂ (or WM–PLA₂) correlations between groups need to take into account the brain structural differences (independent of PLA₂ activity) between compared groups. Indeed, most of our findings of significant GM–PLA₂ or WM–PLA₂ interactions are in clusters, for which we showed a brain structural group difference in GM (or WM, resp.), thus supporting the validity of our interaction findings and the conclusion that these are not just spurious findings but rather relate to the morphological deficit observed in this patient group.

Generally, interaction clusters significant in the FEP vs. controls, as well as the REP vs. controls and FEP vs. REP contrasts are likely to indicate an effect starting early on in the disease and reflect enduring dynamic changes. These apparently enduring changes affect the left prefrontal cortex (Fig. 2, clusters 1 and 25; Fig. 3 cluster 57), left anterior thalamus (Fig. 2, cluster 9; Fig. 3, cluster 64), and bilateral parietal cortices (Table 3a: FEP clusters 7 and 8; REP clusters 27 and 28; Fig. 3: cluster 58, Table 4a: cluster 59). Clusters significant only in the REP vs. healthy controls or the FEP vs. REP contrast, however, rather indicate changes occurring over the course of the disease, or possibly related to either membrane remodelling (i.e. compensation of an initial pathology), or medication or other factors. Clusters with such a profile were observed in the medial orbitofrontal and entorhinal cortex, the left anterior cingulate cortex (Fig. 3, clusters 81 and 83), caudate (Fig. 2, cluster 45; Fig. 3, cluster 84), and cerebellum (Fig. 2, clusters 39 and 49; Fig. 3, clusters 77, 80 and 82). As can be seen for the direct FEP vs. REP comparisons (esp. for gray matter), there are more extensive alterations in the REP group, esp. in areas such as the bilateral frontal cortices (Fig. 2, clusters 25 and 19), inferior parietal cortex (clusters 22, 27, and 28), right posterior thalamus (cluster 35), caudate (cluster 45), and cerebellum (clusters 39 and 49). REP patients do not only show an increased number of affected regions, but these also appear to involve more right hemisphere structures, such as right prefrontal cortex (Fig. 2, cluster 19), right dorsal thalamus (Fig. 2, cluster 35), right parahippocampal gyrus (Fig. 2, cluster 20), superior temporal gyrus (Fig. 3, cluster 62) and temporal pole (Fig. 3, cluster 79).

In the analysis of WM-PLA₂ interactions, we similarly found a number of clusters in regions also showing group-related differences in white matter density, such as the left medial temporal white matter (Fig. 4, cluster 119) and cingulum (Fig. 4, cluster 132; Fig. 5, cluster 159). However, this overlap appears to be less clear than in the GM analyses. In addition, some of the WM interaction clusters overlap with areas of the GM interaction analyses (e.g. left medial temporal regions, anterior cingulate, cerebellum). Notably, the WM analysis in FEP patients shows strong effects in bilateral anterior medial and left dorsolateral thalamic areas, resp. as well as the caudate (Fig. 4, cluster 112).

Depending on disease stage, different GM-PLA₂ (or WM-PLA₂) correlations (positive or negative), and hence different types of interactions with the healthy control group would be expected in different brain regions. This is indeed the fact and can be shown in our results. Comparing FEP and REP to healthy controls, we observed a decrease of gray matter density with increasing PLA₂ activity in several prefrontal/frontal clusters (Fig. 2, clusters 1, 25, and 19). This interaction thus appears to be independent of disease stage or medication effects. Also, these clusters overlap with the finding of lower gray matter density (left medial frontal gyrus) in the VBM comparisons between patients and healthy controls (not taking into account PLA₂ activity). Increased PLA₂ activity in these areas might be related to increase of membrane breakdown, which appears to increase with disease progression (see Fig. 3, FEP vs. REP, clusters 57 and 63; note the regression slope for FEP patients). A similar progression can be assumed for the inferior parietal cortices (Fig. 3, clusters 58 and 59). An opposite effect can be found for the thalamus (Fig. 2; left anterior thalamus in FEP, cluster 9; right dorsolateral in REP, cluster 35), where PLA₂ activity increases with gray matter reduction. There are also regions with a clear difference in the direction of correlations in the FEP vs. REP comparison (as opposed to a mere difference in the correlation coefficients); these are in particular regions in which there are no significant associations in FEP patients vs. controls, such as the anterior cingulate (Fig. 2; clusters 81 and 83), left caudate (cluster 84), and right temporal pole (cluster 79). In these brain areas, the change of correlations between PLA₂ activity and brain structure between patient groups (i.e. shift from FEP to REP patients) can be interpreted as an underlying dynamic process

of adaptation and compensation setting in after disease onset. This might include processes counteracting pathological processes, which are active during the onset of schizophrenia (or the early disease stage), but might also be influenced by environmental and medication factors.

There is evidence from MR spectroscopy studies of neuronal overactivity in the anterior cingulate of FEP, resulting in increased excitotoxic neural membrane breakdown. In REP a different pattern of membrane lipid alterations was found in the anterior cingulate, right prefrontal cortex and left thalamus as compared to left hippocampus and cerebellum, corresponding to our result of different patterns of alterations throughout the brain and dependent on the stage of disorder (Jensen et al., 2002; Jensen et al., 2004). On the other hand, the positive correlations in several cerebellar clusters (Fig. 3, clusters 77 and 80) might be a correlate of the gray matter increase. This is corroborated by ³¹P-MR spectroscopy findings of our group (Smesny et al., 2007; Volz et al., 2000), indicating increase membrane phospholipid turnover in the cerebellum in schizophrenia.

For the WM analyses, we found a pattern with similar heterogeneity of effects or directions of effects. We found only one cluster in the left (to a lesser degree also the right) temporal pole (Fig. 4; clusters 120 and 123) where a decrease in WM was accompanied by an increase in PLA₂ activity. In other areas, we found a positive correlation of WM and PLA₂ activity, which are the thalamus bilaterally, the cerebellar white matter (Fig. 4, FEP vs. controls, clusters 112 and 113; REP vs. controls, cluster 129), as well as the left cingulum white matter (Fig. 4, cluster 132). The comparison of the patient groups, contrasting FEP vs. REP patients, shows a different direction of WM-PLA₂ correlations for several areas, including the right thalamus (Fig. 5, cluster 150), anterior cingulum (Fig. 5, cluster 159), left temporal pole (Fig. 5, cluster 145), as well as the left medial temporal white matter (cluster 149) and right temporal white matter (cluster 161). Overall, however, there appears to be less direct correlation with the VBM analyses of group-related WM differences (without taking into account PLA₂ activity).

Altogether, our findings provide support for the hypothesis that PLA₂ activity modulates gray and white matter structure in schizophrenia. However, the results also demonstrate that the effect size as well as direction of effects is markedly different across regions and between first-episode as opposed to chronic patients. This underlines the fact that PLA₂ activity appears to be involved both in processes of membrane degradation (as part of a core pathophysiology of schizophrenia) and the process of membrane remodelling (as part of the compensation for the pathology, or resilience). Although somewhat inconsistent, ³¹P-MR spectroscopy findings are also suggestive of antipsychotic medication effects on focal membrane lipid metabolism. In prefrontal brain regions, deficits of membrane lipid precursors were found more pronounced in follow-up investigations after antipsychotic treatment (Keshavan et al., 1989). Increased breakdown products of membrane lipids normalized after antipsychotic treatment in prefrontal (Stanley et al., 1995) and temporal (Fukuzako et al., 1999) brain regions. Therefore, the effects in several regions are likely to reflect the different etiology as well as timing of changes in these brain regions. We observed such effects particularly in gray matter, but also in several deep white matter clusters or those at the border of white and gray matter. Besides the well-known areas in the frontal lobe, the orbitofrontal cortex and the anterior cingulate, as well as the thalamus, our findings also include areas that have received less attention, such as the parietal lobes and the cerebellum (although the latter has been increasingly acknowledged for its role in schizophrenia). In those few clusters where we found significant interactions of the PLA₂-GM (or PLA₂-WM) associations, but no effect of diagnosis on GM (or WM, resp.) in VBM analysis, such processes are more difficult to interpret, unless taking into account the possibility of metabolic changes in the absence of detectable structural (group-related) effects. It is interesting to note, however, that metabolic changes in the thalamus in both GM and WM interaction analyses are already detectable in the FEP sample (GM: Fig. 2, cluster 9; WM: Fig. 4,

cluster 12) in the absence of a significant morphometric GM (or WM) difference between FEP and controls.

Finally, we need to consider limitations of our study. Firstly, our biochemical parameter (PLA₂ activity) was obtained from serum. While this might render our enzymatic measures prone to effects of peripheral metabolism, we should point out that our own previous studies in other patient samples have shown robust correlations for these particular types of PLA₂ between samples obtained from CSF and those obtained from peripheral blood samples (Smesny et al., 2009). Secondly, we need to take into account that both PLA₂ and brain morphology are not purely trait-dependent markers, but might also show at least minor state-related variability. For PLA₂, there is sound evidence for increased activity throughout different stages of the disorder, i.e. both in first-episode and chronic patients. We have previously demonstrated this effect to be stronger in first-episode patients and somewhat attenuated, but still significant in chronic patients (Smesny et al., 2005), and this is replicated in the present sample. Similarly, brain morphology shows at least minor state-related changes, for example related to acute psychosis (Garver et al., 2000) or medication (Lieberman et al., 2005). However, such state-related effects, which might affect associations between PLA₂ and brain morphology, would be expected to result rather in loss of effect size or false negative findings. Our interpretation of findings being disease-related is further corroborated by the fact, that we identified VBM–PLA₂ correlations in both schizophrenia groups, but not in the healthy controls, that alterations of different PLA₂ subtypes were reported also in autopsied temporal, prefrontal and occipital cortices and tissue of putamen, hippocampus and thalamus of schizophrenia patients (Ross et al., 1999), and that decreased phospholipids were found also in post mortem tissue of the caudate nucleus (Yao et al., 2000). Thirdly, we need to take into consideration potential age effects, as the patient groups necessarily differed in age. However, including age as a co-variate in the analyses might result in removal of variation that might have been related to disease effects as well. Again, this would rather lead to smaller effects than false positives. To further limit this possibility, we performed all main VBM analyses also without age as co-variate, which resulted in a basically same pattern of findings. Similarly, we also considered the problem of gender distribution as a confounding factor. While we used gender as a co-variate in the general linear models for VBM analyses, certain effects related to skewed distributions of gender in our samples cannot be completely excluded with this approach (our REP group consisted mostly of female patients). For this reason, we also performed a post-hoc analysis with female subjects only. Again, the results basically corroborated the pattern seen in the gender-corrected main analyses. Both post-hoc analyses suggest that neither age nor gender distribution (or the manner of accounting for these effects in the general linear model for VBM) have significantly influenced or even distorted the findings.

In summary, our findings suggest that PLA₂ is directly associated with several brain structural alterations observed in schizophrenia, and that it is therefore likely to provide a biochemical correlate of cellular changes underlying the macroscopic changes in brain morphology that can be observed with VBM. There are marked differences in the direction of correlations, as well as whether the GM–PLA₂ (or WM–PLA₂) associations are detectable in FEP patients only or also in the REP sample, which corroborates our hypothesis that PLA₂ acts not only in a presumed early breakdown of phospholipid membranes, but is also a key element of dynamic changes subsequent to disease progression and its related remodeling of lipid membranes. The identified association with this biochemical marker allows us to better understand the brain structural alterations in schizophrenia as reflecting both static and dynamic processes related to disease pathology.

Role of funding source

The authors declare that the funding sources had no influence on the conception of the study, the analyses, or the drafting of the manuscript.

Financial disclosures and potential conflicts of interests

Neither the first author nor any of the co-authors have received any other financial support than stated in the acknowledgement section. None of the authors has potential conflicts of interest to declare.

Acknowledgments

Dr Smesny was supported by the German Research Foundation (DFG), grant Sm 68/1-1. Prof Lasch was supported by the German Research Foundation (DFG), grant LA 759/5-1. Dr. Gaser was supported by the BMBF, grant 01EV0709.

The authors would like to thank the staff of the Department of Psychiatry of the University of Jena for their extensive support in this study. The authors would also like to thank the staff of the Department of Diagnostic and Interventional Radiology of the University of Jena for their support in obtaining the high-resolution MRI scans.

References

- Andreasen, N.C., Paradiso, S., O'Leary, D.S., 1998. "Cognitive dysmetria" as an integrative theory of schizophrenia: a dysfunction in cortical–subcortical–cerebellar circuitry? *Schizophr. Bull.* 24, 203–218.
- Ashburner, J., Friston, K.J., 2000. Voxel-based morphometry—the methods. *Neuroimage* 11, 805–821.
- Balsinde, J., Balboa, M.A., Insel, P.A., Dennis, E.A., 1999. Regulation and inhibition of phospholipase A2. *Annu. Rev. Pharmacol. Toxicol.* 39, 175–189.
- Berger, G.E., Smesny, S., Amminger, G.P., 2006. Bioactive lipids in schizophrenia. *Int. Rev. Psychiatry* 18, 85–98.
- Chance, S.A., Esiri, M.M., Crow, T.J., 2003. Ventricular enlargement in schizophrenia: a primary change in the temporal lobe? *Schizophr. Res.* 62, 123–131.
- Cuadra, M.B., Cammoun, L., Butz, T., Cuisenaire, O., Thiran, J.P., 2005. Comparison and validation of tissue modelization and statistical classification methods in T1-weighted MR brain images. *IEEE Trans. Med. Imaging* 24, 1548–1565.
- Davis, K.L., Stewart, D.G., Friedman, J.L., Buchsbaum, M., Harvey, P.D., Hof, P.R., Buxbaum, J., Haroutunian, V., 2003. White matter changes in schizophrenia: evidence for myelin-related dysfunction. *Arch. Gen. Psychiatry* 60, 443–456.
- DeLisi, L.E., Sakuma, M., Maurizio, A.M., Relja, M., Hoff, A.L., 2004. Cerebral ventricular change over the first 10 years after the onset of schizophrenia. *Psychiatry Res.* 130, 57–70.
- Dennis, E.A., 1994. Diversity of group types, regulation, and function of phospholipase A2. *J. Biol. Chem.* 269, 13057–13060.
- Falkai, P., Honer, W.G., Alfter, D., Schneider-Axmann, T., Bussfeld, P., Cordes, J., Blank, B., Schonell, H., Steinmetz, H., Maier, W., Tepest, R., 2002. The temporal lobe in schizophrenia from uni- and multiply affected families. *Neurosci. Lett.* 325, 25–28.
- Farooqui, A.A., Yang, H.C., Horrocks, L., 1997a. Involvement of phospholipase A2 in neurodegeneration. *Neurochem. Int.* 30, 517–522.
- Farooqui, A.A., Yang, H.C., Rosenberger, T.A., Horrocks, L.A., 1997b. Phospholipase A2 and its role in brain tissue. *J. Neurochem.* 69, 889–901.
- Farooqui, A.A., Litsky, M.L., Farooqui, T., Horrocks, L.A., 1999. Inhibitors of intracellular phospholipase A2 activity: their neurochemical effects and therapeutic importance for neurological disorders. *Brain Res. Bull.* 49, 139–153.
- Farooqui, A.A., Ong, W.Y., Horrocks, L.A., 2004. Biochemical aspects of neurodegeneration in human brain: involvement of neural membrane phospholipids and phospholipases A2. *Neurochem. Res.* 29, 1961–1977.
- Fukuzako, H., Fukuzako, T., Kodama, S., Hashiguchi, T., Takigawa, M., Fujimoto, T., 1999. Haloperidol improves membrane phospholipid abnormalities in temporal lobes of schizophrenic patients. *Neuropsychopharmacology* 21, 542–549.
- Garver, D.L., 2006. Evolution of antipsychotic intervention in the schizophrenic psychosis. *Curr. Drug Targets* 7, 1205–1215.
- Garver, D.L., Nair, T.R., Christensen, J.D., Holcomb, J.A., Kingsbury, S.J., 2000. Brain and ventricle instability during psychotic episodes of the schizophrenias. *Schizophr. Res.* 44, 11–23.
- Gattaz, W.F., Kollisch, M., Thuren, T., Virtanen, J.A., Kinnunen, P.K., 1987. Increased plasma phospholipase-A2 activity in schizophrenic patients: reduction after neuroleptic therapy. *Biol. Psychiatry* 22, 421–426.
- Gattaz, W.F., Hubner, C.V., Nevalainen, T.J., Thuren, T., Kinnunen, P.K., 1990. Increased serum phospholipase A2 activity in schizophrenia: a replication study. *Biol. Psychiatry* 28, 495–501.
- Gattaz, W.F., Schmitt, A., Maras, A., 1995. Increased platelet phospholipase A2 activity in schizophrenia. *Schizophr. Res.* 16, 1–6.
- Glen, I., Glen, A., 2004. Free radicals don't freeze: why red cell membrane phospholipids stored at low temperatures from schizophrenic patients show increased peroxidation. *Prostaglandins Leukot. Essent. Fatty Acids* 71, 217–219.
- Good, C.D., Johnsrude, I.S., Ashburner, J., Henson, R.N., Friston, K.J., Frackowiak, R.S., 2001. A voxel-based morphometric study of ageing in 465 normal adult human brains. *Neuroimage* 14, 21–36.
- Harrison, P.J., 1999. The neuropathology of schizophrenia. A critical review of the data and their interpretation. *Brain* 122, 593–624.

- Honea, R., Crow, T.J., Passingham, D., Mackay, C.E., 2005. Regional deficits in brain volume in schizophrenia: a meta-analysis of voxel-based morphometry studies. *Am. J. Psychiatry* 162, 2233–2245.
- Horrobin, D.F., Manku, M.S., Hillman, H., Iain, A., Glen, M., 1991. Fatty acid levels in the brains of schizophrenics and normal controls. *Biol. Psychiatry* 30, 795–805.
- Jenkins, C.M., Wolf, M.J., Mancuso, D.J., Gross, R.W., 2001. Identification of the calmodulin-binding domain of recombinant calcium-independent phospholipase A2beta. Implications for structure and function. *J. Biol. Chem.* 276, 7129–7135.
- Jensen, J.E., Al-Semaan, Y.M., Williamson, P.C., Neufeld, R.W., Menon, R.S., Schaeffer, B., Densmore, M., Drost, D.J., 2002. Region-specific changes in phospholipid metabolism in chronic, medicated schizophrenia: 31P-MRS study at 4.0 Tesla. *Br. J. Psychiatry* 180, 39–44.
- Jensen, J.E., Miller, J., Williamson, P.C., Neufeld, R.W., Menon, R.S., Malla, A., Manchanda, R., Schaefer, B., Densmore, M., Drost, D.J., 2004. Focal changes in brain energy and phospholipid metabolism in first-episode schizophrenia: 31P-MRS chemical shift imaging study at 4 Tesla. *Br. J. Psychiatry* 184, 409–415.
- Kasai, K., Shenton, M.E., Salisbury, D.F., Hirayasu, Y., Onitsuka, T., Spencer, M.H., Yurgelun-Todd, D.A., Kikinis, R., Jolesz, F.A., McCarley, R.W., 2003. Progressive decrease of left Heschl gyrus and planum temporale gray matter volume in first-episode schizophrenia: a longitudinal magnetic resonance imaging study. *Arch. Gen. Psychiatry* 60, 766–775.
- Keshavan, M.S., Pettegrew, J.W., Panchalingam, K., Kaplan, D., Brar, J., Campbell, K., 1989. In vivo 31P nuclear magnetic resonance (NMR) spectroscopy of the frontal lobe metabolism in neuroleptic naive first episode psychoses. *Schizophr. Res.* 2, 122.
- Kubicki, M., McCarley, R., Westin, C.F., Park, H.J., Maier, S., Kikinis, R., Jolesz, F.A., Shenton, M.E., 2007. A review of diffusion tensor imaging studies in schizophrenia. *J. Psychiatr. Res.* 41, 15–30.
- Lasch, J., Willhardt, I., Kinder, D., Sauer, H., Smesny, S., 2003. Fluorometric assays of phospholipase A2 activity with three different substrates in biological samples of patients with schizophrenia. *Clin. Chem. Lab. Med.* 41, 908–914.
- Lieberman, J.A., Tollefson, G.D., Charles, C., Zipursky, R., Sharma, T., Kahn, R.S., Keefe, R. S., Green, A.L., Gur, R.E., McEvoy, J., Perkins, D., Hamer, R.M., Gu, H., Tohen, M., 2005. Antipsychotic drug effects on brain morphology in first-episode psychosis. *Arch. Gen. Psychiatry* 62, 361–370.
- Lucas, K.K., Svensson, C.I., Hua, X.Y., Yaksh, T.L., Dennis, E.A., 2005. Spinal phospholipase A2 in inflammatory hyperalgesia: role of group IVA cPLA2. *Br. J. Pharmacol.* 144, 940–952.
- Luders, E., Gaser, C., Narr, K.L., Toga, A.W., 2009. Why sex matters: brain size independent differences in gray matter distributions between men and women. *J. Neurosci.* 29, 14265–14270.
- May, A., Gaser, C., 2006. Magnetic resonance-based morphometry: a window into structural plasticity of the brain. *Curr. Opin. Neurobiol.* 19, 407–411.
- McCarley, R.W., Wible, C.G., Frumin, M., Hirayasu, Y., Levitt, J.J., Fischer, I.A., Shenton, M. E., 1999. MRI anatomy of schizophrenia. *Biol. Psychiatry* 45, 1099–1119.
- Mori, S., Wakana, S., Nagae-Poetscher, L.M., van Zijl, P.C.M., 2005. MRI Atlas of Human White Matter. Elsevier, Amsterdam.
- Nieuwenhuys, R., Voogd, J.N., van Huijzen, C., 2008. The human central nervous system, 4th edition. Springer Verlag, Berlin, London.
- Rajapakse, J.C., Giedd, J.N., Rapoport, J.L., 1997. Statistical approach to segmentation of single-channel cerebral MR images. *IEEE Trans. Med. Imaging* 16, 176–186.
- Reiber, H., 2005. Diagnostics in cerebrospinal fluid. In: Tuber, L. (Ed.), *Diagnosis and laboratory diagnostics - Indication and assessment of laboratory findings in medicine*, pp. 1743–1784. Th- Books.
- Ross, B.M., Hudson, C., Erlich, J., Warsh, J.J., Kish, S.J., 1997. Increased phospholipid breakdown in schizophrenia. Evidence for the involvement of a calcium-independent phospholipase A2. *Arch. Gen. Psychiatry* 54, 487–494.
- Ross, B.M., Turenne, S., Moszczynska, A., Warsh, J.J., Kish, S.J., 1999. Differential alteration of phospholipase A2 activities in brain of patients with schizophrenia. *Brain Res.* 821, 407–413.
- Ross, B.M., Ward, P., Glen, I., 2004. Delayed vasodilatory response to methylnicotinate in patients with unipolar depressive disorder. *J. Affect. Disord.* 82, 285–290.
- Scherk, H., Falkai, P., 2006. Effects of antipsychotics on brain structure. *Curr. Opin. Psychiatry* 19, 145–150.
- Seidman, L.J., Pantelis, C., Keshavan, M.S., Faraone, S.V., Goldstein, J.M., Horton, N.J., Makris, N., Falkai, P., Caviness, V.S., Tsuang, M.T., 2003. A review and new report of medial temporal lobe dysfunction as a vulnerability indicator for schizophrenia: a magnetic resonance imaging morphometric family study of the parahippocampal gyrus. *Schizophr. Bull.* 29, 803–830.
- Shenton, M.E., Dickey, C.C., Frumin, M., McCarley, R.W., 2001. A review of MRI findings in schizophrenia. *Schizophr. Res.* 49, 1–52.
- Smesny, S., Kinder, D., Willhardt, I., Rosburg, T., Lasch, J., Berger, G., Sauer, H., 2005. Increased calcium-independent phospholipase A2 activity in first but not in multi-episode chronic schizophrenia. *Biol. Psychiatry* 57, 399–405.
- Smesny, S., Rosburg, T., Nenadic, I., Fenk, K.P., Kunstmann, S., Rzanny, R., Volz, H.P., Sauer, H., 2007. Metabolic mapping using 2D 31P-MR spectroscopy reveals frontal and thalamic metabolic abnormalities in schizophrenia. *Neuroimage* 35, 729–737.
- Smesny, S., Stein, S., Willhardt, I., Lasch, J., Sauer, H., 2008. Decreased phospholipase A2 activity in cerebrospinal fluid of patients with dementia. *J. Neural Transm.* 115, 1173–1179.
- Song, H., Ramanadham, S., Bao, S., Hsu, F.F., Turk, J., 2006. A bromoenol lactone suicide substrate inactivates group VIA phospholipase A2 by generating a diffusible bromomethyl keto acid that alkylates cysteine thiols. *Biochemistry* 45, 1061–1073.
- Stanley, J.A., Williamson, P.C., Drost, D.J., Carr, T.J., Rylett, R.J., Malla, A., Thompson, R.T., 1995. An in vivo study of the prefrontal cortex of schizophrenic patients at different stages of illness via phosphorus magnetic resonance spectroscopy. *Arch. Gen. Psychiatry* 52, 399–406.
- Steen, R.G., Mull, C., McClure, R., Hamer, R.M., Lieberman, J.A., 2006. Brain volume in first-episode schizophrenia: systematic review and meta-analysis of magnetic resonance imaging studies. *Br. J. Psychiatry* 188, 510–518.
- Sun, G.Y., Xu, J., Jensen, M.D., Simonyi, A., 2004. Phospholipase A2 in the central nervous system: implications for neurodegenerative diseases. *J. Lipid Res.* 45, 205–213.
- Taketo, M.M., Masahiro, S., 2002. Phospholipase A2 and apoptosis. *Biochim. Biophys. Acta* 1585, 72–76.
- Tang, C.Y., Friedman, J., Shungu, D., Chang, L., Ernst, T., Stewart, D., Hajianpour, A., Carpenter, D., Ng, J., Mao, X., Hof, P.R., Buchsbaum, M.S., Davis, K., Gorman, J.M., 2007. Correlations between Diffusion Tensor Imaging (DTI) and Magnetic Resonance Spectroscopy (1H MRS) in schizophrenic patients and normal controls. *BMC Psychiatry* 7, 25.
- Tavares, H., Yacubian, J., Talib, L.L., Barbosa, N.R., Gattaz, W.F., 2003. Increased phospholipase A2 activity in schizophrenia with absent response to niacin. *Schizophr. Res.* 61, 1–6.
- Tohka, J., Zijdenbos, A., Evans, A., 2004. Fast and robust parameter estimation for statistical partial volume models in brain MRI. *Neuroimage* 23, 84–97.
- Tzourio-Mazoyer, N., Landeau, B., Papathanassiou, D., Crivello, F., Etard, O., Delcroix, N., Mazoyer, B., Joliot, M., 2002. Automated anatomical labeling of activations in SPM using a macroscopic anatomical parcellation of the MNI MRI single-subject brain. *Neuroimage* 15, 273–289.
- Velakoulis, D., Wood, S.J., Smith, D.J., Soulsby, B., Brewer, W., Leeton, L., Desmond, P., Suckling, J., Bullmore, E.T., McGuire, P.K., Pantelis, C., 2002. Increased duration of illness is associated with reduced volume in right medial temporal/anterior cingulate grey matter in patients with chronic schizophrenia. *Schizophr. Res.* 57, 43–49.
- Volz, H.R., Riehemann, S., Maurer, I., Smesny, S., Sommer, M., Rzanny, R., Holstein, W., Czekała, J., Sauer, H., 2000. Reduced phosphodiesterases and high-energy phosphates in the frontal lobe of schizophrenic patients: a 31P chemical shift spectroscopic-imaging study. *Biol. Psychiatry* 47, 954–961.
- Weinberger, D.R., Lipska, B.K., 1995. Cortical maldevelopment, anti-psychotic drugs, and schizophrenia: a search for common ground. *Schizophr. Res.* 16, 87–110.
- White, M.C., McHowat, J., 2007. Protease activation of calcium-independent phospholipase A2 leads to neutrophil recruitment to coronary artery endothelial cells. *Thromb. Res.* 120, 597–605.
- Winstead, M.V., Balsinde, J., Dennis, E.A., 2000. Calcium-independent phospholipase A (2): structure and function. *Biochim. Biophys. Acta* 1488, 28–39.
- Wittchen, H.-U., Fydrich, T., Zaudig, M., 1997. *Strukturiertes Klinisches Interview für DSM-IV*. Hogrefe Verlag, Göttingen.
- Yao, J.K., Leonard, S., Reddy, R.D., 2000. Membrane phospholipid abnormalities in postmortem brains from schizophrenic patients. *Schizophr. Res.* 42, 7–17.